

1 **Surface temperature effects of recent reductions in shipping** 2 **SO₂ emissions are within internal variability**

3 Duncan Watson-Parris¹, Laura J. Wilcox², Camilla W. Stjern³, Robert J. Allen⁴, Geeta Persad⁵,
4 Massimo A. Bollasina⁶, Annica M. L. Ekman⁷, Carley E. Iles³, Manoj Joshi⁸, Marianne T.
5 Lund³, Daniel McCoy⁹, and Daniel M. Westervelt¹⁰, Andrew Williams¹¹, Bjørn H. Samset³

6 ¹Scripps Institution of Oceanography and Halıcıoğlu Data Science Institute, UC San Diego

7 ²National Centre for Atmospheric Science, Department of Meteorology, University of Reading

8 ³CICERO Center for International Climate Research, Oslo

9 ⁴Department of Earth and Planetary Sciences, University of California, Riverside

10 ⁵Jackson School of Geosciences, University of Texas at Austin

11 ⁶School of GeoSciences, University of Edinburgh, UK

12 ⁷Department of Meteorology and Bolin Centre for Climate Research, Stockholm University

13 ⁸Climatic Research Unit, School of Environmental Sciences, University of East Anglia, UK

14 ⁹University of Wyoming

15 ¹⁰Lamont-Doherty Earth Observatory, Columbia University

16 ¹¹Princeton University

17 *Correspondence to:* Duncan Watson-Parris (dwatsonparris@ucsd.edu)

18 **Abstract.**

19 In 2020 the International Maritime Organization (IMO) implemented strict new regulations on the emissions of
20 sulphate aerosol from the world's shipping fleet. This can be expected to lead to a reduction in aerosol-driven
21 cooling, unmasking a portion of greenhouse gas warming. The magnitude of the effect is uncertain, however, due
22 to the large remaining uncertainties in the climate response to aerosols. Here, we investigate this question using
23 an 18-member ensemble of fully coupled climate simulations evenly sampling key modes of climate variability
24 with the NCAR CESM2 model. We show that while there is a clear physical response of the climate system to the
25 IMO regulations, including a surface temperature increase, we do not find global mean temperature influence that
26 is significantly different from zero. The 20-year average global mean warming for 2020-2040 is +0.03 °C, with a

27 5-95% confidence range of [-0.09, 0.19], reflecting the weakness of the perturbation relative to internal variability.
28 We do, however, find a robust, non-zero regional temperature response in part of the North Atlantic. We also find
29 that the maximum annual-mean ensemble-mean warming occurs around a decade after the perturbation in 2029,
30 which means that the IMO regulations have likely had very limited influence on observed global warming to date.
31 We further discuss our results in light of other, recent publications that have reached different conclusions. Overall,
32 while the IMO regulations may contribute up to 0.16 °C [-0.17, 0.52] to the global mean surface temperature in
33 individual years during this decade, consistent with some early studies, such a response is unlikely to have been
34 discernible above internal variability by the end of 2023 and is in fact consistent with zero throughout the 2020-
35 2040 period.

36 **Introduction**

37 Anthropogenic aerosols play a complex and dual role in Earth's climate system. On the one hand, they contribute
38 to atmospheric pollution, adversely affecting air quality and public health. On the other hand, they mostly exert a
39 net cooling effect on the climate by increasing the albedo, or reflectivity, of the atmosphere, thereby reducing the
40 amount of solar radiation that reaches the Earth's surface (Bellouin et al., 2020). Sulphate aerosols, for instance,
41 scatter sunlight, directly and enhance cloud brightness by increasing the number of water droplets in clouds, further
42 reflecting sunlight away from the Earth (e.g. Albrecht, 1989; Twomey, 1974). Anthropogenic aerosol emissions
43 thereby currently induce a global average cooling which (partially) offsets greenhouse gas driven warming by
44 around 0.5 [0.22 to 0.96] °C compared to pre-industrial times (Forster et al., 2021). The magnitude of aerosol
45 cooling is a key uncertainty in climate science and hinders our ability to accurately predict the magnitude and
46 timing of future warming (Watson-Parris & Smith, 2022).

47 Environmental and health concerns associated with anthropogenic aerosols have led to international efforts to
48 reduce their emission, with potentially significant consequences for the climate (Wall et al., 2022). In January
49 2020, the International Maritime Organization (IMO) took a significant step in this direction by implementing
50 stringent regulations to curb sulphur dioxide (SO₂; a precursor for sulphate aerosol) emissions from the global
51 shipping fleet (IMO 2019), which at the time contributed around 14% of all anthropogenic sources of these
52 pollutants (Christensen et al., 2022). Given the substantial share of global trade transported by sea, and the
53 corresponding volume of emissions from shipping, the impact of these regulations on the global climate system
54 was anticipated to be notable, and to provide a useful experiment to quantify broader aerosol impacts (Christensen
55 et al., 2022). Similar regulatory efforts in other sectors, and national efforts in major industrial nations such as
56 China (Li et al., 2017; Samset et al., 2019; van der A et al., 2017), also aim to improve air quality by reducing
57 emissions of SO₂ and other aerosol precursors or species, thereby posing a challenge to climate scientists: to
58 quantify and predict how these reductions will influence Earth's energy balance and the ongoing rate and pattern
59 of warming.

60 While focussed studies have found evidence of the effect of the change in shipping emissions on cloud brightness
61 (Diamond, 2023; Watson-Parris et al., 2022), it is challenging to discern any signal in large-scale cloud properties
62 because the observed covariability does not always flow causally from the observed microphysical properties
63 (Glassmeier et al., 2021; Stevens & Feingold, 2009). The instantaneous radiative forcing due to aerosol-cloud
64 interactions from the 2020 change in shipping emissions is estimated to be 0.5 W m⁻² in the annual mean within
65 shipping corridors (Diamond, 2023). Best estimates of the global mean effective radiative forcing (ERF) resulting
66 from an 80% drop in shipping emissions range from 0.035 to 0.15 W m⁻² across multiple models and methodologies
67 (Gettelman et al. 2024; Skeie et al., 2024; Yoshioka et al., 2024). Yuan et al. (2024) report a forcing of 0.2 W m⁻²
68 averaged over the global ocean only, which is consistent with these global estimates.

69

70 A possible discernible climate influence of the IMO regulations became a topic for discussion in 2023, when
71 observed global mean surface temperatures (GMST) set a record. The 2023 GMST anomaly exceeded predictions
72 based on long-term climate change trends and internal variability, including the El Niño-Southern Oscillation
73 (ENSO), by more than 0.2°C, causing speculation that the reduction in SO₂ emissions from shipping could be one
74 of the driving factors (Schmidt, 2024). Based on the estimates of ERF given above, however, calculations with
75 simple energy balance models (EBMs) suggest that the warming associated with shipping changes since 2020 is
76 unlikely to exceed 0.05 °C by 2023, with a long-term response of 0.07°C (Gettelman et al., 2024). A weakness of
77 the EBMs in this case, however, is that they generally assume a spatially homogeneous forcing and thus cannot
78 account for the spatial heterogeneity in ocean feedbacks or climate responses to aerosol forcing, which is known
79 to be substantial (Persad & Caldeira, 2018; Shindell & Faluvegi, 2009; Westervelt et al., 2020).

80

81 To provide a quantitative estimate of the magnitude and pattern of the climate response to the IMO shipping
82 regulations, and the role it may have played in recent record surface temperatures, it is therefore crucial to also
83 have estimates using fully coupled Earth System Models (ESMs), that take into account a broad range of aerosol-
84 climate interactions and their spatial heterogeneity, as well as internal variability and its potential feedback on
85 transient climate forcing. The latter means that it is necessary to use an ensemble of model simulations that is
86 sufficiently large to discern a statistically significant temperature response to a weak perturbation. Even with
87 ESMs, structural uncertainty and ensemble size create disagreement, as evidenced by recent studies of surface
88 warming estimates due to shipping emission reductions. For instance, Yoshioka et al. (2024) found a global mean
89 temperature increase of 0.04°C, averaged over 2020 to 2049, in response to a 0.13 W m⁻² ERF in HadGEM3-

90 GC3.1, while Quaglia & Visioni (2024) found a global temperature increase of 0.2 °C by 2030 in response to an
91 approximately 0.2 W m⁻² radiative perturbation in CESM2 (for a 90% reduction in shipping emissions).

92

93 Here, we present estimates of the transient surface temperature implications of the recent IMO regulations, using
94 a large (18 member) ensemble of fully coupled transient simulations with the Community Earth System Model
95 version 2 (CESM2). We show the ensemble mean response over time and discuss the implications of the sample
96 size for the ability to quantify any forced warming. Also, as it is conceivable that the current specific phases of
97 ENSO and Atlantic Multi-decadal Oscillation (AMO) could be particularly (in)sensitive to radiative perturbations
98 in the shipping corridors (e.g. Wang et al., 2022), we have designed the ensemble to sample different modes of
99 climate variability. Finally, as there have already been a range of studies quantifying the temperature response to
100 the IMO regulations leading to differing, if not opposite, conclusions, we provide a broader discussion on the
101 challenges and limitations of disentangling the effect of shipping emissions using currently available climate
102 modelling methodologies.

103 **Methods**

104 CESM2 (Danabasoglu et al., 2020) consists of the Community Atmosphere Model version 6 (CAM6; Bogenschutz
105 et al., 2018), the Parallel Ocean Program version 2 (POP2; Danabasoglu et al., 2012), the Community Land Model
106 version 5 (CLM5; Lawrence et al., 2019), and the Community Ice Code version 5 (CICE; Hunke et al., 2015).
107 Aerosols in CAM6 are represented by the four-mode version of the Modal Aerosol Module (MAM4; Liu et al.,
108 2016). We note that 2.5% of SO₂ emissions from the international shipping sector are emitted as sulphate aerosol
109 at the surface level and into the accumulation mode (Emmons et al., 2020). The cloud microphysics scheme is

110 version 2 of the Morrison-Gottelman scheme (Gottelman & Morrison, 2015). Simulations are performed at
111 approximately 1° horizontal resolution.

112

113 Our baseline experiments come from archived simulations performed as part of the CESM2 Large Ensemble
114 (CESM2-LE) Project (Rodgers et al., 2021). From 2015 onwards, CESM2-LE uses aerosol/precursor gas
115 emissions (including SO₂/SO₄ from international shipping), land use changes, and greenhouse gas concentrations
116 from the Shared Socioeconomic Pathway 3-7.0 (SSP3-7.0; O'Neill et al., 2016). Our perturbation experiments are
117 initialised from the CESM2-LE baseline experiments beginning in 2015 and integrated through 2040. The
118 perturbation simulations are identical to the baseline simulations, except for a uniform 80% reduction in SO₂/SO₄
119 emissions from international shipping starting in 2020 (consistent with the IMO regulations) and extending through
120 2040. Thus, taking a difference (perturbation minus baseline) isolates the effects of the decrease in SO₂ emissions
121 from international shipping.

122

123 CESM2 has a relatively strong anthropogenic aerosol forcing when quantified in isolation, and a high climate
124 sensitivity compared to other ESMs (see Figure 1; Schlund et al., 2020; Zelinka et al., 2023). Its oceanic response
125 has also been shown to be particularly sensitive to aerosol emissions (Fasullo et al., 2023; Hassan et al., 2021).
126 For this particular perturbation however, CESM2 shows a similar radiative forcing to other ESMs (Skeie et al.,
127 2024). Our model setup is the same as the one used for CESM2 in Gottelman et al. 2024 who report an ERF of
128 0.11 Wm⁻² for a 100±25% reduction in shipping SO₂ emissions. This places CESM2 near the mean of the ERF
129 estimates recently provided (Skeie et al., 2024; Gottelman et al. 2024).

130

131 To help understand the possible importance of the imposed shipping emissions perturbation relative to internal
132 climate variability, we perform 18 ensemble simulations. These ensemble members all use CESM2-LE
133 realisations that feature 11-year running mean smoothed CMIP6 biomass burning emissions, including members
134 1011-001, 1031-002, 1051-003, 1091-005, 1111-006, 1131-007, 1151-008, 1171-009, 1191-010, 1231-011, 1231-
135 012, 1231-016, 1231-018, 1251-012, 1281-017, 1281-020, 1301-015, 1301-017. All comparisons and differences
136 are calculated with respect to the 18 corresponding unperturbed ensemble members. Recent satellite data
137 introduces more interannual variability into the biomass burning dataset than data sources used before 1997 and
138 after 2014, so smoothing reduces the variability in biomass burning fluxes over 1990–2020 (Fasullo et al., 2022).
139 Furthermore, to help understand the possible importance of dominant modes of climate variability (e.g., ENSO
140 and AMV) to the climate impacts associated with the shipping perturbation, 8 of the above ensemble members
141 feature ENSO neutral conditions, 5 feature ENSO positive conditions and 5 feature ENSO negative conditions.
142 The AMV index is also evenly sampled in the ensemble, for each ENSO state, and spans -0.15 to 0.15.

143

144 The simulated responses are compared to observed SST changes, diagnosed from the HadCRUT v5.0.2 analysis
145 (Morice et al., 2021). We fit a locally weighted regression (LOESS) model over time to each 5x5 degree grid-cell
146 to model the long-term SST trends (2020-2040), and then subtract this to discern the anomaly in 2023.

147

148 In the following, unless otherwise specified, estimates for surface temperature change are for the period 2020-
149 2040. All significance tests are performed using a two-sided Student’s t-test for the null hypothesis that two
150 independent samples (drawn from two distributions with equal variance) have identical average (expected) values.

151 **Results**

152 Figure 2a shows the relative change in near-surface SO₂ concentration in the reduction scenario compared to
153 baseline and demonstrates that the majority of the changes in near-surface SO₂ occur over the Northern Hemisphere
154 oceans and in particular over the North Atlantic and North-East Pacific – clearly aligned with the main international
155 shipping routes. Figure 2b shows the change in near-surface SO₂ concentrations over the simulation period both
156 globally and over the North Atlantic. The gradual reduction in the change over the period is due to the underlying
157 shipping emission reductions in the baseline SSP3-7.0 scenario.

158
159 Despite these wide-spread and regionally significant changes in SO₂ concentrations (and corresponding SO₄
160 concentrations, not shown), the temperature response in these simulations is negligible. Based on our sample of
161 18 simulations, we calculate a global, 20-year mean surface temperature change from the IMO regulations of +0.03
162 °C, with a 5-95% confidence range of [-0.09, 0.19]. Figure 3a shows the temperature change with respect to the
163 baseline simulations as a global mean and over the North Atlantic, neither of which show significant spatial-mean
164 warming over the 20-year study period. In fact, over the first five years there is no statistically robust change in
165 temperature found anywhere on the globe (see Fig 3b), demonstrating the low strength of the perturbation with
166 respect to the model’s simulated internal variability of the Earth system. Averaging over 20 years, a robust
167 localized signal starts to appear during 2020-2040 in a small region of the North Atlantic (see Fig 3c) where there
168 is a statistically significant local warming of around 0.2°C. Figure 3d shows that the anomalous warming observed
169 in the region in 2023 (see Methods) does broadly correspond with the pattern of simulated warming in response to
170 the IMO regulations, but only as discerned after 20 years, visualised in Fig. 3e (which is a close-up of 3c).

171

172 Despite some degree of similarity between the recent observed anomalous warming and the simulated temperatures
173 shown in Fig 3e, the timescales do not match. The observed anomalies occurred three years after the emissions
174 changes, while the average model response over the first five years (2020-2025) shows no significant warming in
175 the region (Fig. 3b). As noted above, it is possible that the particular phase of ENSO or AMO could have made
176 the North Atlantic particularly susceptible to such a perturbation in this short period of time in observations, but
177 by sub-sampling our ensemble based on these characteristic modes we still find no evidence that the shipping
178 emissions changes could have contributed significantly to the observed global temperature changes (see Fig. 4).

179

180 As mentioned above, detecting the climate impacts of a relatively small externally forced perturbation, such as the
181 estimated global top-of-atmosphere radiative forcing associated with the IMO shipping regulations (e.g., $+0.12 \pm 0.03$ Wm^{-2} ; Gettelman et al. 2024), is complicated by the influence of internal climate variability (Deser et al.,
182 2012, 2020). Figure 5 shows the actual evolution of our 18 ensemble members, with and without the IMO
183 regulations, compared to the HadCRUT5 global surface temperature anomaly data series. The observed evolution
184 is clearly within the range sampled by CESM2, in both emission scenarios. This difficulty is compounded over
185 smaller (e.g., regional) spatial scales and shorter (e.g., decadal) time scales. The ability to robustly separate and
186 quantify a forced signal in the climate system is the goal and motivation of “large-ensembles” (e.g. Kay et al.,
187 2015; Kirchmeier-Young et al., 2017; Maher et al., 2019; Rodgers et al., 2021; Simpson et al., 2023), whereby
188 dozens or more independent climate model ensemble members are generated using identical external forcing but
189 different initial climate states. Since ensemble members will in general feature different timing of internal climate
190 variability—which essentially represents noise (i.e., the component of the signal that is not externally forced)—
191 averaging over a larger number of ensemble members reduces such noise, allowing for a more robust quantification
192 of the externally forced signal.

193

194

195 Figure 6 shows the important influence of internal climate variability to the global mean temperature response (ΔT)
196 in our CESM2 shipping perturbation experiments, as well as the importance of having a sufficient ensemble size
197 to robustly detect a forced response. Fig. 6a shows the impact of randomly selecting N of our 18 ensemble
198 members with replacement (i.e. a bootstrapping analysis). For each combination we calculate the corresponding
199 ensemble global mean temperature response. The figure shows the results from 1000 samples. For small N , the
200 spread in the ensemble mean ΔT is quite large (approximately -0.09 to 0.125 °C for $N = 5$). For $N = 10$, the spread
201 is reduced, but it still exceeds ± 0.05 °C. As N continues to increase, however, the spread converges to our 18-
202 ensemble member ΔT .

203

204 To further illustrate the importance of ensemble size when dealing with perturbations that have weak responses
205 relative to internal variability, Figure 6b-d show example combinations of 10 unique ensemble members (as used
206 e.g. by Quaglia & Visoni, 2024). Statistical testing and hatching is done as for our Figure 3 (see Methods). Fig.
207 6b shows a 10-member combination consistent with our 18-member mean response ($\Delta T = 0.03$ °C). 6c and 6d
208 show 10-member combinations with ΔT at the edges of, but still within, the 9-95% confidence interval ($\Delta T = \pm 0.05$
209 °C).

210

211 While panels b-d of Figure 6 all represent deliberate picking of ensemble members, the analysis illustrates how,
212 even with a decently sized ensemble of 10 members, one could conclude that the IMO shipping regulations may
213 lead to substantial global mean warming or global mean cooling. This illustrates the importance of internal climate
214 variability in detecting a global mean temperature response associated with the IMO shipping regulations, and the
215 importance of a sufficiently large ensemble size to reduce the risk of spurious conclusions. We note that our choice

216 of 18 ensemble members, as with most experimental designs, also represents a trade-off between additional
217 information gained versus increased computational expense. Clearly, however, a moderately large ensemble size
218 of 10—which has been shown to be sufficient in some contexts (e.g. Monerie et al., 2022)—is not sufficient to
219 make robust claims regarding the impact of shipping SO₂ reductions on global mean temperature, in particular
220 during its early transient evolution.

221

222 **Discussion and conclusions**

223 The strict new fuel regulations introduced by the IMO provided a valuable experiment to better understand the
224 role of changing anthropogenic aerosol in the climate system, particularly as an analogue to other, current and
225 future, efforts to improve air quality globally. Using an 18-member ensemble of simulations from CESM2, we
226 find that the global temperature response to the IMO regulations that came into force in 2020 is +0.03 °C, with a
227 5-95% confidence range of [-0.09, 0.19], for the period 2020-2040. This result, which is consistent with a null
228 hypothesis of no discernible global mean temperature response, is at the low end of other estimates of this warming
229 effect, from simple energy balance models (Gettelman et al., 2024; Yuan et al., 2024) and global climate models
230 (Quaglia & Visioni, 2024; Yoshioka et al., 2024), which suggested global warming between 0.04 °C (Yoshioka et
231 al., 2024) and 0.2 °C (Quaglia & Visioni, 2024) associated with the shipping regulations over decadal timescales.
232 To understand the differences between these conclusions and to explain why our analysis provides an important
233 bound on the role of shipping emissions changes in recently observed temperature extremes, it is necessary to
234 discuss in some detail the methodologies and framings behind the other results.

235

236 Some recent studies of the climate impact of the IMO regulations used EBMs to calculate the global temperature
237 response from the effective radiative forcing (Gettelman et al., 2024; Yuan et al., 2024). These simple models are
238 useful in many situations, notably for comparing the climate implications of known emissions from industrial
239 sectors, regions or scenarios. However for absolute climate impacts they require substantial assumptions to be
240 made about the sensitivity and timescale of the responses, and – critically - do not account for regional
241 heterogeneity of responses or climate feedbacks such as influences on ocean circulation or sea ice, or internal
242 variability. Ocean feedbacks may be particularly important in the case of shipping emission changes which are
243 focussed over the Northern Hemisphere oceans, where it is conceivable that the ocean mixed layers may warm
244 more efficiently than e.g. the Southern Ocean (e.g. Ma et al., 2020). Region-specific cloud responses and
245 teleconnections to aerosol changes over Northern Hemisphere oceans may also differ from those to e.g. sulphur
246 emission changes in Asia (Burney et al., 2022; Persad & Caldeira, 2018), which tend to dominate the total global
247 response to recent sulphur emission changes used to calibrate simple EBMs. Coupled climate models provide
248 estimates of the temperature response to the IMO regulations that take such feedbacks and pattern dependencies
249 into account.

250

251 Despite the differences in the approach, our estimate of the global warming due to the IMO regulations is similar
252 to Gettelman et al. (2024)'s estimate of 0.07 °C by 2030, which is based on the FaIR EBM. The EBM approach
253 taken by Yuan et al. (2024), however, which diagnoses a global temperature anomaly of 0.17 °C at equilibrium
254 overstates the response to their forcing by a factor of 1.4. This is because Yuan et al. (2024) calculate a global
255 temperature response using a global climate feedback parameter, but using an ocean-area mean ERF. A global
256 feedback parameter should be used with a global forcing in this context, which would reduce their forcing and
257 temperature estimates by a factor of 0.7, the fraction of global area that is ocean, from 0.2 W m⁻² to 0.14 W m⁻²

258 and 0.17 °C to 0.12 °C in equilibrium, respectively. Uncertainty in the climate feedback parameter should also be
259 considered in this estimate. Using a feedback parameter equivalent to that of CO₂, the AR6 likely range for ECS
260 of 2.5-4.0 °C (which may both be oversimplistic assumptions), and 2xCO₂ forcing of 3.9±0.5 W m⁻² (90% range)
261 would produce an equilibrium warming due to a forcing of 0.14 W m⁻² of 0.09-0.14 °C (90% range). Seven years,
262 the timescale used by Yuan et al. (2024) in their calculation, is approximately the time taken for the upper-ocean
263 to reach equilibrium, so, based on Gregory et al. (2024), one would expect to see around two thirds of the
264 equilibrium response (i.e. 0.06-0.10 °C) in that time. With these factors taken into account, the estimate presented
265 by Yuan et al. (2024) would have been consistent with those of Gettelman et al. (2024), and those presented in this
266 work.

267
268 ESM estimates of the temperature response to the IMO regulations initially appear to show similar diversity to
269 those based on EBMs. However, this can be seen to largely be due to a difference in the framing of the experiments
270 and reporting of the results, rather than a substantive difference in the main conclusions. Using HadGEM3-GC3.1-
271 LL, Yoshioka et al. (2024) estimated a global mean warming of 0.04 °C (averaged over 2020-2049), which is in
272 agreement with our estimate of 0.03 [-0.09,0.19] °C (averaged over 2020-2040). Their model has a similar ERF
273 of 0.13 Wm⁻², and they use coupled transient simulations with 12 ensemble members per experiment. Their global
274 mean warming estimate is similar to that presented in this study, but the pattern of warming is markedly different,
275 with most of the significant warming over SE Asia and the East Pacific. Conversely, Quaglia & Vioni (2024)
276 estimate a temperature increase of 0.2 °C by 2030 due to the introduction of the IMO regulations. They use the
277 same model that we have used in this study, and a similar experiment design, with transient simulations initialised
278 from the CESM2 Large Ensemble. Although their temperature response is an order of magnitude larger than our
279 stated response, it is not inconsistent with our results. We show in Figure 3a that the global temperature response

280 to the reduction of shipping emissions peaks in 2029 at 0.16 [-0.17, 0.52] °C. Our best estimate of the warming by
281 2030 is 0.07 [-0.14, 0.28] °C, where the range is ± 1 standard deviation and encompasses a warming of 0.2 °C.
282 However, our 18-member ensemble shows that the global ensemble mean warming over 2020-2040 is not
283 statistically significantly different from zero ($p=0.18$), even in 2030 ($p=0.054$).

284

285 The apparently large discrepancy between our CESM2 numbers and those from Quaglia & Visioni (2024) also
286 demonstrates the importance of framing. We report a 2020-2040 mean value, and they report the value for 2030.
287 Both our Figure 3a and Yoshioka et al. (2024)'s Figure 6 show that the maximum global temperature response to
288 the 2020 emissions change occurs around 2030, and the estimate of the temperature response by 2030 is consistent
289 across all three studies. Yoshioka et al. (2024) also find a long-term mean response of 0.04 °C, averaged over
290 2020-2049, which is more consistent with our estimate of 0.03 °C. However, while we show in Figure 3a that the
291 global warming in response to the IMO regulations is not significant, Yoshioka et al. (2024) present significant
292 decadal mean warming in their Figure 6. However, this is based on ± 1 standard error (SE), while we show ± 1
293 standard deviation. Yoshioka et al. (2024) use 12 members, so their standard deviation of $\sqrt{12} * SE$ would also
294 indicate that these decadal mean values were always within one standard deviation of 0, consistent with our results.

295

296 Using large ensembles of simulations differing only by the initial conditions is an important technique for
297 distinguishing forced responses from internal variability, particularly when looking for regional responses, or
298 considering small forcings. Here, our large ensemble confirms that the global response to IMO regulations in
299 CESM2 cannot be distinguished from internal variability, at least in terms of global mean surface temperature.
300 Our best estimate is not significantly different from zero, and subsampling our 18-member ensemble to produce
301 estimates of the global temperature response based on different ensemble sizes always returns a mean estimate

302 that is not significantly different from 0 at the 5% level. In fact, given the ensemble variance and the number of
303 simulations available, the minimum detectable effect size over the full 20 years at a significance level of 0.05 is
304 approximately 0.048 °C. The warming due to the ship emissions changes in CESM2 is therefore very likely less
305 than 0.05 °C. A 10-member ensemble, as used by Quaglia & Visoni (2024), can only significantly detect an effect
306 larger than 0.07 °C. To demonstrate this, 10 members sub-sampled from within our 18-member ensemble, can
307 give a global warming estimate of 0.05 °C or a global cooling of 0.05 °C, averaged over 2020-2040.

308

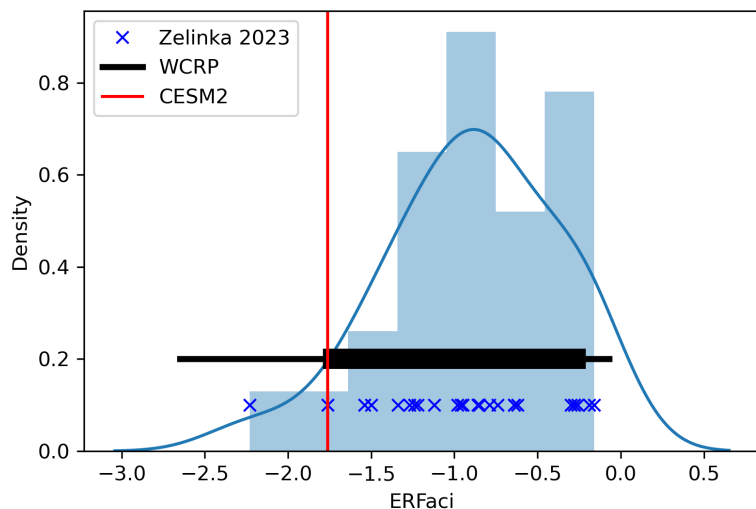
309 Large ensembles also make it possible to characterise the spatial pattern of the response, and identify physically
310 robust responses that are consistent across ensemble members. North Atlantic, Greenland Iceland and Norwegian
311 (GIN) seas, South Atlantic, and East Pacific warming are common features of all our subsampled ensembles.
312 However, only the North Atlantic and GIN sea warming are physically robust in addition to being significant at
313 the 5% level. The difference between the pattern of warming shown in this work and by Yoshioka et al. (2024)
314 likely has a large component of internal variability, in addition to the effects of structural differences between the
315 models used.

316

317 Our results highlight the challenge in rapidly attributing observed extreme events to evolving or temporary
318 anthropogenic changes, particularly given the large internal climate variability on annual-to-decadal timescales.
319 By crowd-sourcing computing resources we were able to rapidly generate an ensemble of fully coupled Earth
320 System Model simulations of sufficient size to quantify the forced response and its confidence interval. However,
321 this highlights a deficiency in current medium term climate attribution tasks. As climate change is broadly
322 acknowledged to be increasingly contributing to the extreme events experienced by millions of people around the
323 world, climate scientists are increasingly tasked with understanding and accurately attributing them - but the

324 resources to conduct this at scale are limited and ad-hoc. An operational climate body that was specifically tasked
325 with running decadal-scale attribution studies (Stevens 2024), or the development of trusted methods for separating
326 forced signals from variability (Samset et al. 2022), would provide a valuable resource as the demand for such
327 information accelerates. The IMO shipping regulations do lead to a relatively small forced global mean surface
328 warming in on our results, consistent with its moderate aerosol ERF, and also with a zero response when internal
329 variability is taken into account. However, we note that other, future and ongoing, broader aerosol emission
330 reductions — although uncertain (Persad et al., 2023) — are expected to lead to a much larger aerosol ERF (e.g.,
331 Wilcox et al., 2023) and may thus still drive significant global warming and regional climate change impacts (e.g.,
332 Allen et al., 2020; Allen et al., 2021).

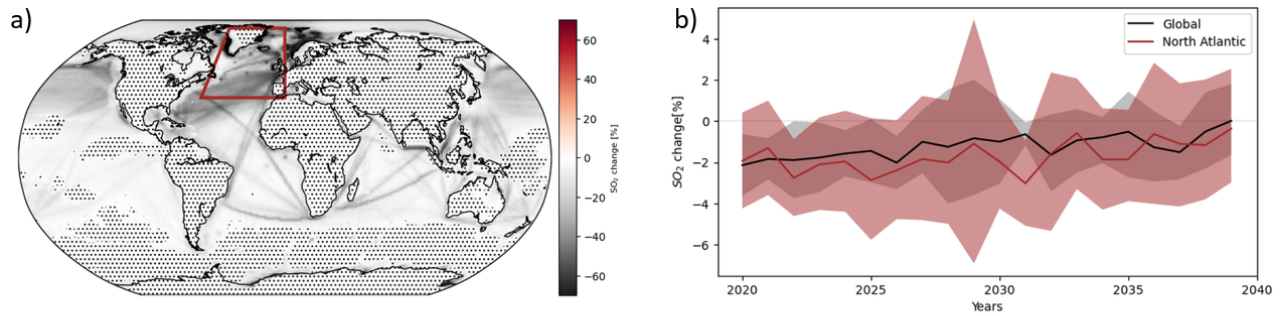
333 Figures



334

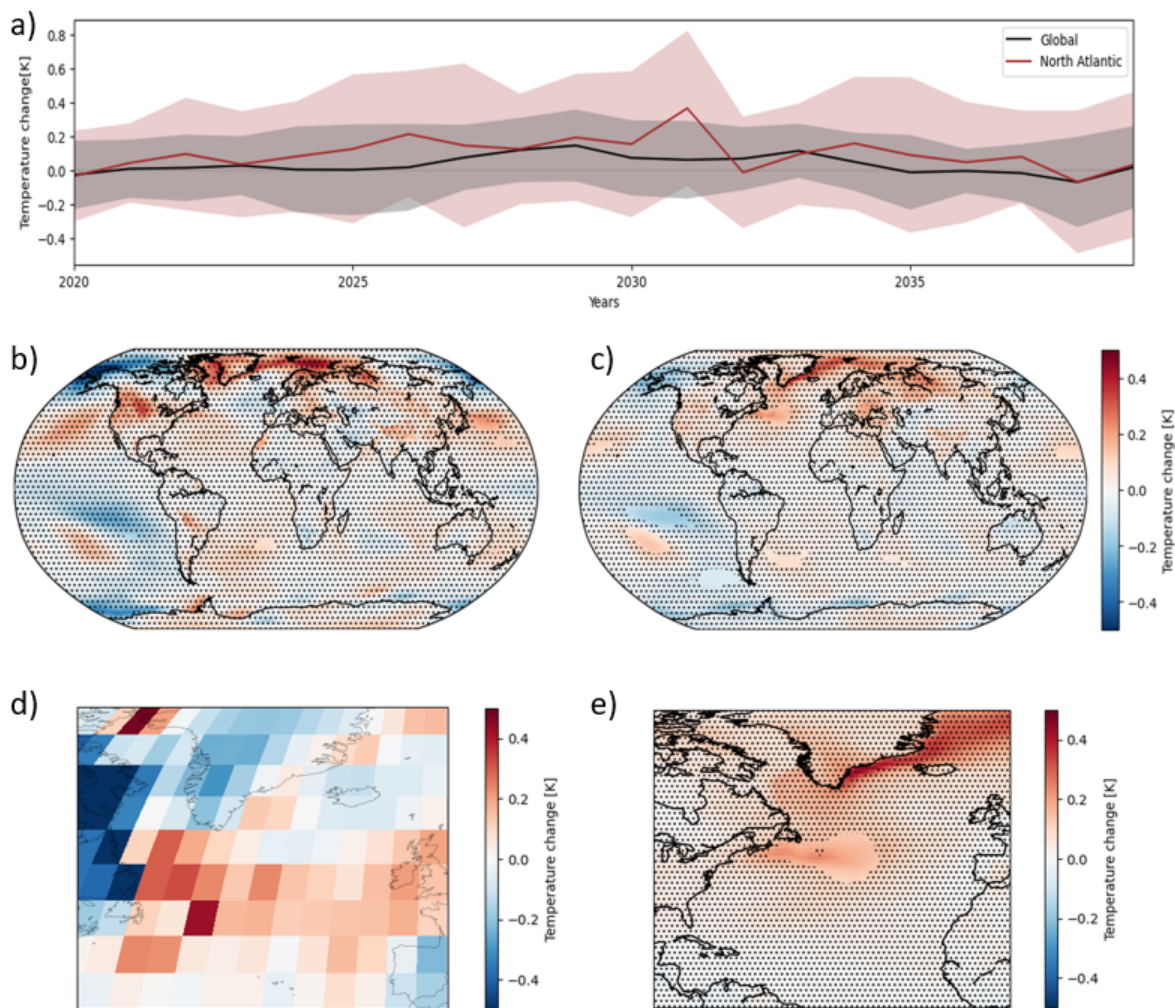
335 **Figure 1: Distribution of the effective radiative forcing due to aerosol cloud interactions (ERFaci) in CMIP6 models as**
336 **assessed by Zelinka et al. (2023) in blue, and Bellouin et al. 2020 in black, with CESM2 highlighted in red.**

337



338

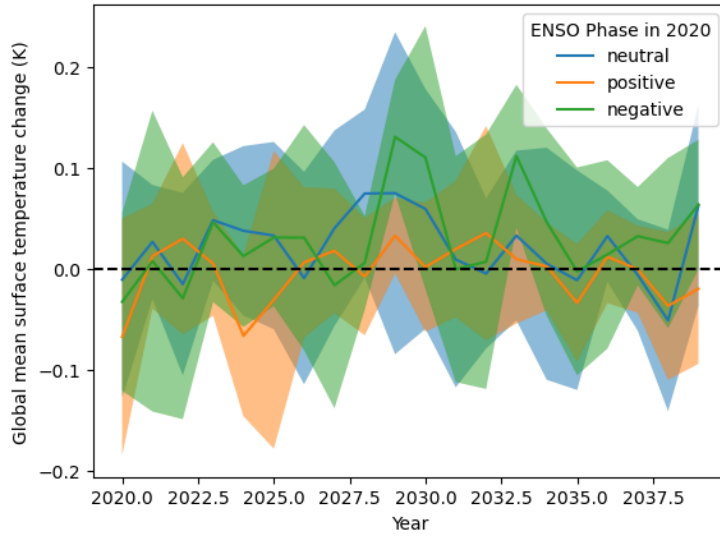
339 **Figure 2: a) Relative change in SO₂ near the surface due to the shipping emissions perturbation, averaged over the**
340 **whole 2020-2040 period, where stippling represents locations where the null hypothesis of ‘no change’ cannot be**
341 **rejected at P < 0.05. b) Annual mean evolution of SO₂, averaged over the entire globe (black line; shading shows +/- one**
342 **standard deviation in ensemble member spread) and over the North Atlantic region (red line) as indicated on the map.**
343 **All changes are relative to the baseline Shared Socioeconomic Pathway 3-7.0 (SSP370).**



344

345 **Figure 3: a) Global and North Atlantic annual mean evolution in temperature change (shading shows +/- one standard**
 346 **deviation in ensemble member spread); b) Annual mean temperature change for 2020-2025; c) Annual mean**
 347 **temperature change for 2020-2040; d) Observed anomalous warming in North Atlantic sea-surface temperature in**
 348 **2023; e) A close-up of (c) showing the corresponding region of the North Atlantic. Stippling in b,c,e represents locations**
 349 **where the null hypothesis of ‘no change’ cannot be rejected at $P < 0.05$. All changes are relative to the corresponding**
 350 **baseline CESM2 LENS simulations of SSP370.**

351



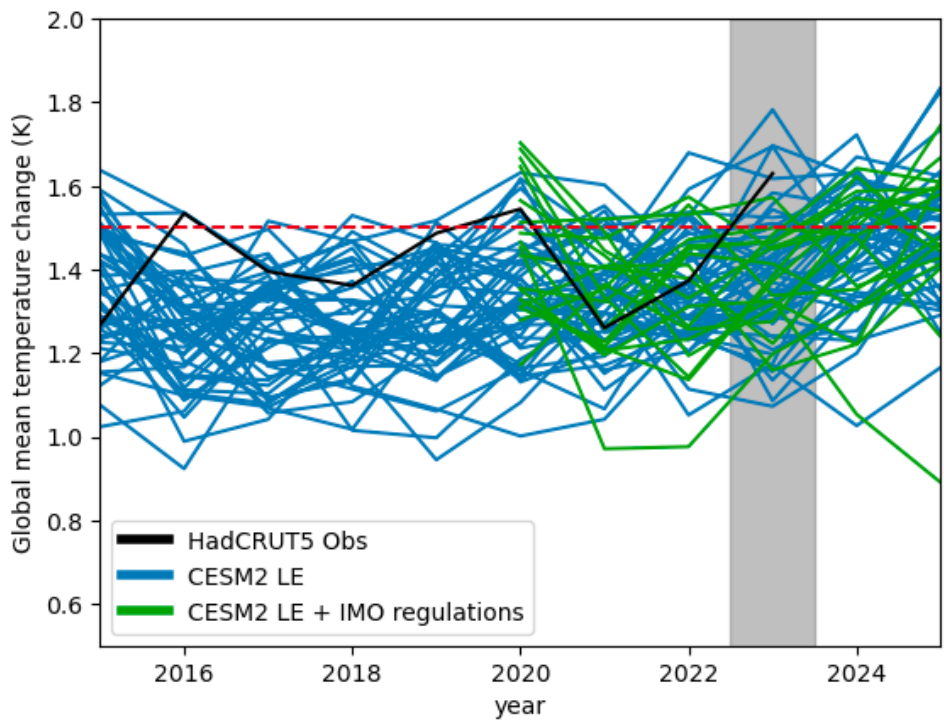
352

353 **Figure 4: Global mean change in surface temperature due to shipping emissions changes with respect to the baseline**

354 **SSP370 simulations, subdivided into three ENSO phases in 2020: neutral (blue; 8 members); positive (orange; 5**

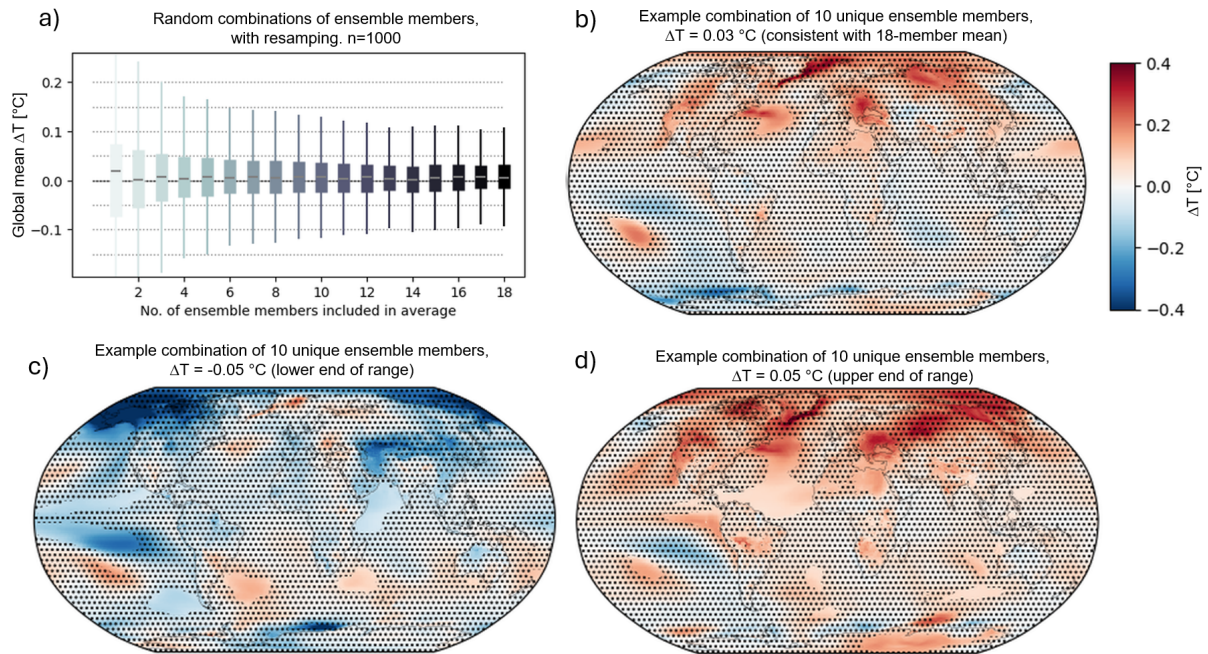
355 **members); negative (green; 5 members). Shading shows the inter-member spread, represented by +/- one standard**

356 **deviation.**



357

358 **Figure 5: Global mean surface temperature change with respect to piControl for the baseline historical + SSP370**
 359 **CESM2 LENS ensemble (blue) and the perturbed shipping emissions ensemble performed in this study (green), overlaid**
 360 **on the HadCRUT SST observational estimate (with respect to the 1850-1900 average; black). The year 2023 is**
 361 **highlighted. The red dashed line represents the 1.5°C Paris agreement warming threshold.**



362
 363 **Figure 6: Ensemble size is crucial for quantifying a forced signal for weak perturbations. (a) Spread in 2020-2040 global,**
 364 **annual mean surface temperature change (ΔT) when randomly sampling and averaging N (given on the x-axis) ensemble**
 365 **members out of the total of 18 available members 1000 times, with resampling. Each spread includes 1000 combinations,**
 366 **illustrating an increasing robustness of ΔT as number of ensemble members. Boxes show the median and 5-95% range,**
 367 **whiskers show the maximum and minimum values. (b) Example combination of 10 ensemble members, where the**
 368 **global, annual mean ΔT is consistent with the 18-member mean ($\Delta T = 0.03^{\circ}\text{C}$). Hatching shows grid points not**
 369 **significant at the 95% confidence level, as for Figure 2. (c) As panel (c), but for an example combination consistent with**
 370 **ΔT at the lower end of the 10-member mean range. ($\Delta T = -0.05^{\circ}\text{C}$). (d) As panel (c), but for an example combination**
 371 **consistent with ΔT at the upper end of the 10-member mean range. ($\Delta T = 0.05^{\circ}\text{C}$).**

372

373 **Competing Interests**

374 At least one of the (co-)authors is a member of the editorial board of Atmospheric Chemistry and Physics.
375

376 **Acknowledgements**

377 Part of the simulations were enabled by resources provided by the National Academic Infrastructure for
378 Supercomputing in Sweden (NAISS), partially funded by the Swedish Research Council through grant agreement
379 no. 2022-06725. B.H.S, C.W.S, L.J.W. and M.T.L. acknowledge funding by the Research Council of Norway
380 through projects CATHY (324182), and support by the Center for Advanced Study in Oslo, Norway that funded
381 and hosted the HETCLIF centre during the academic year of 2023/24. C.W.S. is also supported by the Research
382 Council of Norway through the ACCEPT project (315195). G.P acknowledges support from the U.S. National
383 Science Foundation under AGS-CLD Award #2235177. A.M.L.E acknowledges support from the European
384 Union's Horizon 2020 research and innovation programme (FORCeS, grant no. 821205). R.J.A. is supported by
385 NSF grant AGS-2153486. We would like to acknowledge high-performance computing support from Cheyenne
386 (doi:10.5065/D6RX99HX) provided by the NCAR-Wyoming Supercomputing Center, sponsored by the National
387 Science Foundation and the State of Wyoming and supported by NCAR's Computational and Information Systems
388 Laboratory using allocation WYOM0182. The authors are grateful to Jonathan Gregory for discussions that
389 strengthened this manuscript.

390

391

392

393

394
395
396
397
398
399
400
401
402
403
404
405
406
407
408
409
410
411
412
413
414
415

References

Albrecht, B. A. (1989). Aerosols, Cloud Microphysics, and Fractional Cloudiness. *Science*, 245(4923), 1227–1230. <https://doi.org/10.1126/science.245.4923.1227>

Bellouin, N., Quaas, J., Gryspeerdt, E., Kinne, S., Stier, P., Watson-Parris, D., Boucher, O., Carslaw, K. S., Christensen, M., Daniau, A.-L., Dufresne, J.-L., Feingold, G., Fiedler, S., Forster, P., Gettelman, A., Haywood, J. M., Lohmann, U., Malavelle, F., Mauritsen, T., ... Stevens, B. (2020). Bounding Global Aerosol Radiative Forcing of Climate Change. *Reviews of Geophysics*, 58(1), e2019RG000660. <https://doi.org/10.1029/2019RG000660>

Bogenschutz, P. A., Gettelman, A., Hannay, C., Larson, V. E., Neale, R. B., Craig, C., & Chen, C.-C. (2018). The path to CAM6: coupled simulations with CAM5.4 and CAM5.5. *Geoscientific Model Development*, 11(1), 235–255. <https://doi.org/10.5194/gmd-11-235-2018>

Burney, J., Persad, G., Proctor, J., Bendavid, E., Burke, M., & Heft-Neal, S. (2022). Geographically resolved social cost of anthropogenic emissions accounting for both direct and climate-mediated effects. *Science Advances*, 8(38), eabn7307. <https://doi.org/10.1126/sciadv.abn7307>

Christensen, M. W., Gettelman, A., Cermak, J., Dagan, G., Diamond, M., Douglas, A., Feingold, G., Glassmeier, F., Goren, T., Grosvenor, D. P., Gryspeerdt, E., Kahn, R., Li, Z., Ma, P. L., Malavelle, F., McCoy, I. L.,

416 McCoy, D. T., McFarquhar, G., Mülmenstädt, J., ... Yuan, T. (2022). Opportunistic experiments to constrain
417 aerosol effective radiative forcing. *Atmospheric Chemistry and Physics*, 22(1), 641–674.
418 <https://doi.org/10.5194/acp-22-641-2022>

419 Danabasoglu, G., Bates, S. C., Briegleb, B. P., Jayne, S. R., Jochum, M., Large, W. G., Peacock, S., & Yeager, S.
420 G. (2012). The CCSM4 Ocean Component. *Journal of Climate*, 25(5), 1361–1389.
421 <https://doi.org/10.1175/JCLI-D-11-00091.1>

422 Danabasoglu, G., Lamarque, J.-F., Bacmeister, J., Bailey, D. A., DuVivier, A. K., Edwards, J., Emmons, L. K.,
423 Fasullo, J., Garcia, R., Gettelman, A., Hannay, C., Holland, M. M., Large, W. G., Lauritzen, P. H., Lawrence,
424 D. M., Lenaerts, J. T. M., Lindsay, K., Lipscomb, W. H., Mills, M. J., ... Strand, W. G. (2020). The
425 Community Earth System Model Version 2 (CESM2). *Journal of Advances in Modeling Earth Systems*,
426 12(2), e2019MS001916. <https://doi.org/https://doi.org/10.1029/2019MS001916>

427 Deser, C., Knutti, R., Solomon, S., & Phillips, A. S. (2012). Communication of the role of natural variability in
428 future North American climate. *Nature Climate Change*, 2(11), 775–779.
429 <https://doi.org/10.1038/nclimate1562>

430 Deser, C., Lehner, F., Rodgers, K. B., Ault, T., Delworth, T. L., DiNezio, P. N., Fiore, A., Frankignoul, C., Fyfe,
431 J. C., Horton, D. E., Kay, J. E., Knutti, R., Lovenduski, N. S., Marotzke, J., McKinnon, K. A., Minobe, S.,
432 Randerson, J., Screen, J. A., Simpson, I. R., & Ting, M. (2020). Insights from Earth system model initial-
433 condition large ensembles and future prospects. *Nature Climate Change*, 10(4), 277–286.
434 <https://doi.org/10.1038/s41558-020-0731-2>

435 Diamond, M. S. (2023). Detection of large-scale cloud microphysical changes within a major shipping corridor
436 after implementation of the International Maritime Organization 2020 fuel sulfur regulations. *Atmospheric
437 Chemistry and Physics*, 23(14), 8259–8269. <https://doi.org/10.5194/acp-23-8259-2023>

438 Emmons, L. K., Schwantes, R. H., Orlando, J. J., Tyndall, G., Kinnison, D., Lamarque, J.-F., Marsh, D., Mills, M.
439 J., Tilmes, S., Bardeen, C., Buchholz, R. R., Conley, A., Gettelman, A., Garcia, R., Simpson, I., Blake, D.
440 R., Meinardi, S., & Pétron, G. (2020). The Chemistry Mechanism in the Community Earth System Model
441 Version 2 (CESM2). *Journal of Advances in Modeling Earth Systems*, 12(4), e2019MS001882.
442 <https://doi.org/10.1029/2019MS001882>

443 Fasullo, J. T., Lamarque, J.-F., Hannay, C., Rosenbloom, N., Tilmes, S., DeRepentigny, P., Jahn, A., & Deser, C.
444 (2022). Spurious Late Historical-Era Warming in CESM2 Driven by Prescribed Biomass Burning
445 Emissions. *Geophysical Research Letters*, 49(2), e2021GL097420. <https://doi.org/10.1029/2021GL097420>

446 Fasullo, J. T., Rosenbloom, N., & Buchholz, R. (2023). A multiyear tropical Pacific cooling response to recent
447 Australian wildfires in CESM2. *Science Advances*, 9(19), eadg1213. <https://doi.org/10.1126/sciadv.adg1213>

448 Forster, P., Storelvmo, T., Armour, K., Collins, W., Dufresne, J.-L., Frame, D., Lunt, D., Mauritsen, T., Palmer,
449 M., & Watanabe, M. (2021). The Earth's energy budget, climate feedbacks, and climate sensitivity. *Climate
450 Change 2021: The Physical Science Basis. Contribution of Working Group I to the Sixth Assessment Report
451 of the Intergovernmental Panel on Climate Change*, 923–1054. <https://doi.org/10.1017/9781009157896.009>

452 Gettelman, A., & Morrison, H. (2015). Advanced Two-Moment Bulk Microphysics for Global Models. Part I:
453 Off-Line Tests and Comparison with Other Schemes. *Journal of Climate*, 28(3), 1268–1287.
454 <https://doi.org/10.1175/JCLI-D-14-00102.1>

455 Gettelman, A., Christensen, M. W., Diamond, M. S., Gryspeerd, E., Manshausen, P., Stier, P., Watson-Parris,
456 D., Yang, M., Yoshioka, M., Yuan, T.: Has Reducing Ship Emissions Brought Forward Global Warming?
457 *Geophysical Review Letters* (under review)

458 Glassmeier, F., Hoffmann, F., Johnson, J. S., Yamaguchi, T., Carslaw, K. S., & Feingold, G. (2021). Aerosol-
459 cloud-climate cooling overestimated by ship-track data. *Science*, 371(6528), 485–489.
460 <https://doi.org/doi:10.1126/science.abd3980>

461 Hassan, T., Allen, R. J., Liu, W., & Randles, C. A. (2021). Anthropogenic aerosol forcing of the Atlantic
462 meridional overturning circulation and the associated mechanisms in CMIP6 models. *Atmospheric*
463 *Chemistry and Physics*, 21(8), 5821–5846. <https://doi.org/10.5194/acp-21-5821-2021>

464 Hunke, E. C., Lipscomb, W. H., Turner, A. K., Jeffery, N., & Elliott, S. (2015). CICE: the Los Alamos Sea Ice
465 Model Documentation and Software User’s Manual Version 5. *Los Alamos National Laboratory Technical*
466 *Report, LA-CC-06-012*.

467 IMO: IMO 2020: Consistent Implementation of MARPOL Annex VI. International Maritime Organization, 2019

468 Kay, J. E., Deser, C., Phillips, A., Mai, A., Hannay, C., Strand, G., Arblaster, J. M., Bates, S. C., Danabasoglu, G.,
469 Edwards, J., Holland, M., Kushner, P., Lamarque, J.-F., Lawrence, D., Lindsay, K., Middleton, A., Munoz,
470 E., Neale, R., Oleson, K., ... Vertenstein, M. (2015). The Community Earth System Model (CESM) Large
471 Ensemble Project: A Community Resource for Studying Climate Change in the Presence of Internal Climate
472 Variability. *Bulletin of the American Meteorological Society*, 96(8), 1333–1349.
473 <https://doi.org/10.1175/BAMS-D-13-00255.1>

474 Kirchmeier-Young, M. C., Zwiers, F. W., & Gillett, N. P. (2017). Attribution of Extreme Events in Arctic Sea Ice
475 Extent. *Journal of Climate*, 30(2), 553–571. <https://doi.org/10.1175/JCLI-D-16-0412.1>

476 Lawrence, D. M., Fisher, R. A., Koven, C. D., Oleson, K. W., Swenson, S. C., Bonan, G., Collier, N., Ghimire,
477 B., van Kampenhout, L., Kennedy, D., Kluzek, E., Lawrence, P. J., Li, F., Li, H., Lombardozzi, D., Riley,
478 W. J., Sacks, W. J., Shi, M., Vertenstein, M., ... Zeng, X. (2019). The Community Land Model Version 5:

479 Description of New Features, Benchmarking, and Impact of Forcing Uncertainty. *Journal of Advances in*
480 *Modeling Earth Systems*, 11(12), 4245–4287. <https://doi.org/10.1029/2018MS001583>

481 Li, C., McLinden, C., Fioletov, V., Krotkov, N., Carn, S., Joiner, J., Streets, D., He, H., Ren, X., Li, Z., &
482 Dickerson, R. R. (2017). India Is Overtaking China as the World’s Largest Emitter of Anthropogenic Sulfur
483 Dioxide. *Scientific Reports*, 7(1), 14304. <https://doi.org/10.1038/s41598-017-14639-8>

484 Liu, X., Ma, P. L., Wang, H., Tilmes, S., Singh, B., Easter, R. C., Ghan, S. J., & Rasch, P. J. (2016). Description
485 and evaluation of a new four-mode version of the Modal Aerosol Module (MAM4) within version 5.3 of the
486 Community Atmosphere Model. *Geoscientific Model Development*, 9(2), 505–522.
487 <https://doi.org/10.5194/gmd-9-505-2016>

488 Ma, X., Liu, W., Allen, R. J., Huang, G., & Li, X. (2020). Dependence of regional ocean heat uptake on
489 anthropogenic warming scenarios. *Science Advances*, 6(45). <https://doi.org/10.1126/sciadv.abc0303>

490 Maher, N., Milinski, S., Suarez-Gutierrez, L., Botzet, M., Dobrynin, M., Kornblueh, L., Kröger, J., Takano, Y.,
491 Ghosh, R., Hedemann, C., Li, C., Li, H., Manzini, E., Notz, D., Putrasahan, D., Boysen, L., Claussen, M.,
492 Ilyina, T., Olonscheck, D., ... Marotzke, J. (2019). The Max Planck Institute Grand Ensemble: Enabling the
493 Exploration of Climate System Variability. *Journal of Advances in Modeling Earth Systems*, 11(7), 2050–
494 2069. <https://doi.org/10.1029/2019MS001639>

495 Monerie, P.-A., Wilcox, L. J., & Turner, A. G. (2022). Effects of Anthropogenic Aerosol and Greenhouse Gas
496 Emissions on Northern Hemisphere Monsoon Precipitation: Mechanisms and Uncertainty. *Journal of*
497 *Climate*, 35(8), 2305–2326. <https://doi.org/10.1175/JCLI-D-21-0412.1>

498 Morice, C. P., Kennedy, J. J., Rayner, N. A., Winn, J. P., Hogan, E., Killick, R. E., Dunn, R. J. H., Osborn, T. J.,
499 Jones, P. D., & Simpson, I. R. (2021). An Updated Assessment of Near-Surface Temperature Change From

500 1850: The HadCRUT5 Data Set. *Journal of Geophysical Research: Atmospheres*, 126(3).
501 <https://doi.org/10.1029/2019JD032361>

502 O’Neill, B. C., Tebaldi, C., Vuuren, D. P. van, Eyring, V., Friedlingstein, P., Hurtt, G., Knutti, R., Kriegler, E.,
503 Lamarque, J.-F., Lowe, J., Meehl, G. A., Moss, R., Riahi, K., & Sanderson, B. M. (2016). The Scenario
504 Model Intercomparison Project (ScenarioMIP) for CMIP6. *Geoscientific Model Development*, 9(9), 3461–
505 3482. <https://doi.org/https://doi.org/10.5194/gmd-9-3461-2016>

506 Persad, G. G., & Caldeira, K. (2018). Divergent global-scale temperature effects from identical aerosols emitted
507 in different regions. *Nat Commun*, 9(1), 3289. <https://doi.org/10.1038/s41467-018-05838-6>

508 Quaglia, I., & Vioni, D. (2024). Modeling 2020 regulatory changes in international shipping emissions helps
509 explain 2023 anomalous warming. *EGUsphere*, 1–19. <https://doi.org/10.5194/egusphere-2024-1417>

510 Rodgers, K. B., Lee, S.-S., Rosenbloom, N., Timmermann, A., Danabasoglu, G., Deser, C., Edwards, J., Kim, J.-
511 E., Simpson, I. R., Stein, K., Stuecker, M. F., Yamaguchi, R., Bódai, T., Chung, E.-S., Huang, L., Kim, W.
512 M., Lamarque, J.-F., Lombardozzi, D. L., Wieder, W. R., & Yeager, S. G. (2021). Ubiquity of human-
513 induced changes in climate variability. *Earth System Dynamics*, 12(4), 1393–1411.
514 <https://doi.org/10.5194/esd-12-1393-2021>

515 Samset, B. H., Lund, M. T., Bollasina, M., Myhre, G., & Wilcox, L. (2019). Emerging Asian aerosol patterns.
516 *Nature Geoscience*, 12(8), 582–584. <https://doi.org/10.1038/s41561-019-0424-5>

517 Schlund, M., Lauer, A., Gentine, P., Sherwood, S. C., & Eyring, V. (2020). Emergent constraints on equilibrium
518 climate sensitivity in CMIP5: do they hold for CMIP6? *Earth System Dynamics*, 11(4), 1233–1258.
519 <https://doi.org/10.5194/esd-11-1233-2020>

520 Schmidt, G. (2024). Climate models can’t explain 2023’s huge heat anomaly — we could be in uncharted territory.
521 *Nature*, 627(8004), 467. <https://doi.org/10.1038/d41586-024-00816-z>

522 Shindell, D., & Faluvegi, G. (2009). Climate response to regional radiative forcing during the twentieth century.
523 *Nature Geoscience*, 2(4), 294–300. <https://doi.org/10.1038/ngeo473>

524 Simpson, I. R., Rosenbloom, N., Danabasoglu, G., Deser, C., Yeager, S. G., McCluskey, C. S., Yamaguchi, R.,
525 Lamarque, J.-F., Tilmes, S., Mills, M. J., & Rodgers, K. B. (2023). The CESM2 Single-Forcing Large
526 Ensemble and Comparison to CESM1: Implications for Experimental Design. *Journal of Climate*, 36(17),
527 5687–5711. <https://doi.org/10.1175/JCLI-D-22-0666.1>

528 Skeie, R. B., Byrom, R., Hodnebrog, Ø., Jouan, C., & Myhre, G. (2024). Multi-model effective radiative forcing
529 of the 2020 sulphur cap for shipping. *EGUsphere*, 1–14. <https://doi.org/10.5194/egusphere-2024-1394>

530 Stevens, B., & Feingold, G. (2009). Untangling aerosol effects on clouds and precipitation in a buffered system.
531 *Nature*, 461(7264), 607–613. <https://doi.org/10.1038/nature08281>

532 Twomey, S. (1974). Pollution and the planetary albedo. *Atmospheric Environment (1967)*, 8(12), 1251–1256.
533 <http://www.sciencedirect.com/science/article/pii/0004698174900043>

534 van der A, R. J., Mijling, B., Ding, J., Koukouli, M. E., Liu, F., Li, Q., Mao, H., & Theys, N. (2017). Cleaning up
535 the air: effectiveness of air quality policy for SO₂ and NO_x emissions in China. *Atmospheric Chemistry and*
536 *Physics*, 17(3), 1775–1789. <https://doi.org/10.5194/acp-17-1775-2017>

537 Wall, C. J., Norris, J. R., Possner, A., McCoy, D. T., McCoy, I. L., & Lutsko, N. J. (2022). Assessing effective
538 radiative forcing from aerosol–cloud interactions over the global ocean. *Proceedings of the National*
539 *Academy of Sciences*, 119(46), e2210481119. <https://doi.org/10.1073/pnas.2210481119>

540 Wang, G., Cai, W., Santoso, A., Wu, L., Fyfe, J. C., Yeh, S.-W., Ng, B., Yang, K., & McPhaden, M. J. (2022).
541 Future Southern Ocean warming linked to projected ENSO variability. *Nature Climate Change*, 12(7), 649–
542 654. <https://doi.org/10.1038/s41558-022-01398-2>

543 Watson-Parris, D., Christensen, M. W., Laurenson, A., Clewley, D., Gryspeerdt, E., & Stier, P. (2022). Shipping
544 regulations lead to large reduction in cloud perturbations. *Proceedings of the National Academy of Sciences*,
545 *119*(41), e2206885119. <https://doi.org/10.1073/pnas.2206885119>

546 Watson-Parris, D., & Smith, C. J. (2022). Large uncertainty in future warming due to aerosol forcing. *Nature*
547 *Climate Change*, *12*(12), 1111–1113. <https://doi.org/10.1038/s41558-022-01516-0>

548 Westervelt, D. M., Mascioli, N. R., Fiore, A. M., Conley, A. J., Lamarque, J.-F., Shindell, D. T., Faluvegi, G.,
549 Previdi, M., Correa, G., & Horowitz, L. W. (2020). Local and remote mean and extreme temperature
550 response to regional aerosol emissions reductions. *Atmospheric Chemistry and Physics*, *20*(5), 3009–3027.
551 <https://doi.org/https://doi.org/10.5194/acp-20-3009-2020>

552 Yoshioka, M., Grosvenor, D. P., Booth, B. B. B., Morice, C. P., & Carslaw, K. S. (2024). Warming effects of
553 reduced sulfur emissions from shipping. *EGUsphere*, 1–19. <https://doi.org/10.5194/egusphere-2024-1428>

554 Yuan, T., Song, H., Oreopoulos, L., Wood, R., Bian, H., Breen, K., Chin, M., Yu, H., Barahona, D., Meyer, K., &
555 Platnick, S. (2024). Abrupt reduction in shipping emission as an inadvertent geoengineering termination
556 shock produces substantial radiative warming. *Communications Earth & Environment*, *5*(1), 1–8.
557 <https://doi.org/10.1038/s43247-024-01442-3>

558 Zelinka, M. D., Smith, C. J., Qin, Y., & Taylor, K. E. (2023). Comparison of methods to estimate aerosol effective
559 radiative forcings in climate models. *Atmospheric Chemistry and Physics*, *23*(15), 8879–8898.
560 <https://doi.org/10.5194/acp-23-8879-2023>

561

562

563